Preprints of the 19th World Congress
The International Federation of Automatic Control
Cape Town, South Africa. August 24-29, 2014

Model-based Rack Force Estimation for Electric Power Steering

Steve Fankem * **Thomas Weiskircher** * **Steffen Müller** **

* *Institute for Mechatronics in Mechanical and Automotive Engineering, University of Kaiserslautern, D-67663 Kaiserslautern, Germany (e-mail: steve.fankem@mv.uni-kl.de, thomas.weiskircher@mv.uni-kl.de).*
** *Fachgebiet Kraftfahrzeuge, TU Berlin, D-10623 Berlin, Germany (e-mail: steffen.mueller@tu-berlin.de).*

Abstract: In modern cars, hydraulic power steering (HPS) is continuously substituted by the electric power steering (EPS), active front steering (AFS) or steer-by-wire (SbW). In general, the main task of the EPS/HPS is the support of the driver in controlling the lateral position of the car and compensating the tyre aligning torques. These torques result in a steering rack force, which reliable long-term measurement induces disadvantages e.g. high sensor costs. Since the knowledge of the steering rack force is useful to improve various automotive control applications, the estimation of the steering rack force with real-time capable algorithms is in the focus of this research. First, a non-linear dynamic 4-mass model is given and validated by a prototype EPS. Second, an algorithm for steering rack force estimation is introduced using a non-linear friction compensation module and a linear disturbance observer. Finally, the estimation algorithm is analysed by means of validated numerical EPS model, a steering test bench and a real prototype car. The results state the excellent performance of the estimation algorithm, even under real operation conditions.

Keywords: steering rack force estimation, steering actuator design, electric power steering

1. INTRODUCTION

Considering all actuators of modern cars, the steering system is the most important one to design the feedback to the driver and the vehicle manoeuvrability. Additionally, an innovative steering device enables various driver assist functions e.g. lane keeping systems or side wind assist. With the additional requirements of future cars as energy consumption, the conventional hydraulic power steering is substituted by novel electric powered steering systems. These lead to more precise control of the steering functions and improved energy efficiency of the steering device. Besides, various types of steering devices like active front steering (AFS) or steer-by-wire (SbW) must be considered when new assist functions are developed. A detail analyse of the EPS structure states that extended functionality is possible with the common steering system sensors e.g. the current-based torque sensor of the power assist motor and the steering wheel position sensor. Additional to the driver and the power assist torque of the steering system, the tyre-road contact forces are important for various applications, since they include information about the tyre contact behaviour to the road. This information is necessary to design a realistic steering wheel feedback, see Fankem et al. [2013], Hsu et al. [2013]. Secondly, this information is useful for vehicle dynamics control since it supports the improvement of road friction estimation, see Weiskircher et al. [2012], Hsu [2010]. Moreover, the knowledge of the steering rack force is helpful to improve the SbW position control performance by the use of a closed loop controller with disturbance rejection. To support these different functions, this paper presents a model-based algorithm for real-time estimation of the steering rack force. This is generated by the tyre aligning torques and the link of the tyres to the steering rack via the tie rods. Hence in general, two main methods for model-based estimation of the steering rack force are possible. The first one uses a detailed vehicle dynamics model to calculate the tyre aligning torques and the kinematic description of the linkage to the steering rack to estimate the rack force, see Koch [2010], Weiskircher et al. [2012]. The disadvantage of this method is the comprehensive parameter requirement for the vehicle and the complex tyre-ground interaction, e.g. vehicle mass and suspension kinematics, tyre side stiffness, road grade, and road slope. Thus, this method is difficult to apply to production cars. Alternatively, an actuation-based estimation using the sensors of the steering system only, is a more promising method, as the actuator has a minor parameter uncertainty as the vehicle. Therefore, this research concentrates on the second method and introduces a model-based estimation of the reaction force. In this paper, the widely spread rack assist electric power steering system (EPS) is used to analyse the functionality of the estimation algorithm. First, a detailed system description including system dynamics modelling is given. The validation is done by the help of a real prototype EPS mounted on a steering test-bench. Afterward, a non-linear algorithm to estimate the rack force is proposed. Finally, the algorithm is validated by the detailed system model, the steering system test bench and a pre-production car.

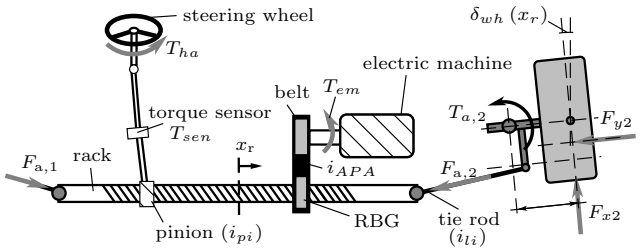

Fig. 1. Rack assist EPS structure and definitions

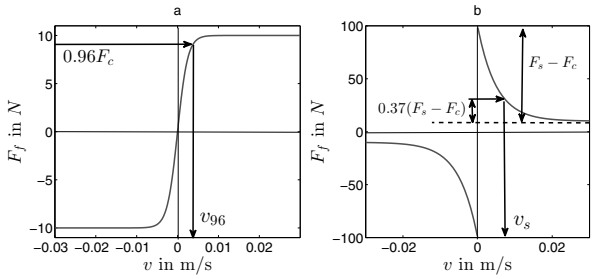

Fig. 2. Definitions for the non-linear friction force model

2. MODELING OF THE ELECTRIC POWER STEERING (EPS)

In this section, a general model of the EPS is proposed and analysed. The electric motor is connected to the steering rack via a drive belt and a recirculating ball gear (RBG), see Fig. 1. The steering rack is then linked to the road wheels by the tie rods and the driver input is transferred to the steering rack by the steering wheel and the steering column. Consequently, the torque between the steering column and the pinion is measured by a torque sensor to allow for the calculation of power assist functions (Hsu et al. [2013]).

2.1 Description of the EPS system dynamics

Fig. 1 shows the complete steering mechanics for at least two kinds of systems: a rack assist EPS as well as a SbW wheel actuator if the steering column is blanked out. Thus, a mathematical model of the EPS includes one more mass, named J_{sw}. As can be seen in Fig. 1, 3 inputs act on the mechanics: the column torque, the electric motor torque with delay T_t and time constant τ_{em}, and the rack force F_r. To achieve the mathematical description of the steering model, the equivalent 5-mass system in Fig. 3 is used. This includes all physical parts of the system: the steering column with the steering wheel (sw), the torque sensor (sen), the wheel and suspension inertia J_{wh}, the rack, the screw ball (ba) and its stiffness and damping, the belt (be) stiffness and damping, the rotor (rot) of the electric motor (em) and the dynamics of the motor control. Additionally, the parameter m_r describes the steering rack mass and J_{ba} the inertia of the RBG. The last part, J_{ro} includes the electric motor and the drive belt. The part J_{wh} of the road wheels and the moving parts of the suspension are assumed to be linked to the rack by the tie rods with the ratio $i_{li}(x_r)$. Using $i_{li}(x_r)$, a 4-mass model can be derived with $m_2(i_{li})$ as the resulting mass of the rack and the suspension, which depends on the rack position

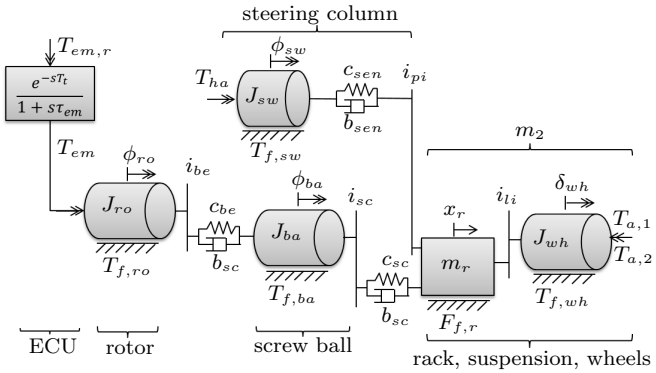

Fig. 3. Equivalent 5-mass steering system structure

as given in eq. (1e). For this reason, the equations of the dynamic 4-mass steering model with motor dynamics and the definitions in eq. (1)

$$\phi_1 = \phi_{sw}, \qquad x_2 = x_r \tag{1a}$$
$$\phi_3 = \phi_{ba}, \qquad \phi_4 = \phi_{ro} \tag{1b}$$
$$J_1 = J_{sw}, \qquad J_3 = J_{ba} \tag{1c}$$
$$J_4 = J_{ro}, \qquad v_2 = \dot{x}_2 \tag{1d}$$
$$m_2 = m_r + i_{li}^2(x_2)\, J_{wh} = f(x_2) \tag{1e}$$
$$i_{be} = \dot{\phi}_{ro}/\dot{\phi}_{ba}, \quad i_{sc} = \dot{\phi}_{ba}/v_r \tag{1f}$$
$$i_{APA} = i_{be} i_{scr} = \dot{\phi}_{ro}/v_r, \quad i_{pi} = \dot{\phi}_{sw}/v_r \tag{1g}$$

read

$$\begin{aligned} J_1\ddot{\phi}_1 &= T_{ha} - T_{f,1} - c_{sen}(\phi_1 - i_{pi}x_2) \\ &\quad - b_{sen}\left(\dot{\phi}_1 - i_{pi}\dot{x}_2\right) \end{aligned} \tag{2a}$$
$$\begin{aligned} m_2\ddot{x}_2 &= -F_r - F_{f,2} + i_{pi}c_{sen}(\phi_1 - i_{pi}x_2) \\ &\quad + i_{pi}b_{sen}\left(\dot{\phi}_1 - i_{pi}\dot{x}_2\right) + c_{sc}(\phi_3/i_{sc} - x_2) \\ &\quad + b_{sc}\left(\dot{\phi}_3/i_{sc} - \dot{x}_2\right) \end{aligned} \tag{2b}$$
$$\begin{aligned} J_3\ddot{\phi}_3 &= -T_{f,3} - (1/i_{sc})\, c_{sc}(\phi_3/i_{sc} - x_2) \\ &\quad - (1/i_{sc})\, b_{sc}\left(\dot{\phi}_3/i_{sc} - \dot{x}_2\right) + c_{be}(\phi_4/i_{be}\phi_3) \\ &\quad + b_{be}\left(\dot{\phi}_4/i_{be} - \dot{\phi}_3\right) \end{aligned} \tag{2c}$$
$$\begin{aligned} J_4\ddot{\phi}_4 &= T_{em} - T_{f,4} - (1/i_{be})\, c_{be}(\phi_4/i_{be} - \phi_3) \\ &\quad - (1/i_{be})\, b_{be}\left(\dot{\phi}_4/i_{be} - \dot{\phi}_3\right) \end{aligned} \tag{2d}$$
$$\dot{T}_{em} = 1/\tau_{em}\left(-T_{em} + T_{em,r}(t - T_t)\right). \tag{2e}$$

with the steering wheel torque T_{ha}. The interesting rack force

$$F_r = F_{a,1} + F_{a,2} \tag{3}$$

is resulting from the tie rod reaction forces $F_{a,q}$, $q \in (1,2)$, which are generated by the road wheel aligning torques $T_{a,q}$. As tyre and suspension parameters only influence the absolute value of aligning torque transferred to the tie rods but not the rack force itself, no direct knowledge of them is required. In addition, the friction torques $T_{f,i}$ and force $F_{f,i}$ are modelled as a combination of static friction F_s, dry friction F_c, Stribeck friction, and viscous friction between the moving parts, the mounting points and the bearings:

$$T_{f,i} = \left(T_{c,i} + (T_{s,i} - T_{c,i}) \exp - \frac{\left|\dot{\phi}_i\right|}{\dot{\phi}_{s,i}} \right) \tanh \left(\frac{2}{\dot{\phi}_{96,i}} \dot{\phi}_i \right) + b_i \dot{\phi}_i, \quad i \in (1,3,4) \tag{4}$$

$$F_{f,2} = \left(F_{c,2} + (F_{s,2} - F_{c,2}) \exp - \frac{|v_i|}{v_{s,2}} \right) \tanh \left(\frac{2}{v_{96,2}} v_2 \right) + b_2 v_2. \tag{5}$$

The parameters $v_{s,2}$, $v_{96,2}$, $\dot{\phi}_{s,i}$ and $\dot{\phi}_{96,i}$ are assumed to be independent of absolute part positions as often seen in dynamic friction models. Herein, v_{96} is the velocity at which 96 % of the maximum amplitude of the friction force is reached in case of dry friction only and v_s is the velocity when the difference between static and dry friction is reduced by 63 %, see Fig. 2. Thus, for the validation of the EPS model, these parameters need to be identified in addition to the system mass, inertia, stiffness, and damping values.

2.2 Validation of the steering dynamics model

Before the steering dynamics model of the previous section can be used for the rack force estimation, the parameters of the real system are required. Therefore, a preproduction series EPS is mounted on a test-bench and identified by different test manoeuvres. As a series EPS normally uses the electric motor to support the driver by specialised algorithms for different operation points, the power assist functions are disabled and the motor reference torque $T_{em,r}$ is directly transmitted to the ECU by a CAN controller of the test-bench real-time hardware. Five different results are analysed. First, the test-bench measurements of the real EPS and the results of the proposed 4-mass model are presented. Additionally, different reduced order models with three, two and only one mass are shown. The torque sinus sweep signal to the EPS ECU is in the frequency range from 0 Hz to 3 Hz. The selection of the degree of freedom (DOF) for the reduced mass systems depends on the parameters of the system and the frequency range of interest, see Dannöhl et al. [2012]. Assuming a rigid connection between the RCG and the rack, the 4-mass model is reduced to a 3-mass model, while the two mass system is the result of a rigid connection between rotor and RBG with the belt drive. Finally, an 1-mass model is found assuming a rigid link between column and rack. Thus, for all reduced order models, the inertia result of the reduction with the given ratio between the masses in Fig. 3. Fig. 4 gives an idea about the performance of the model in time domain up to 3 Hz. As no clear difference is visible, Fig. 5 states the validity of reduced models up to 15 Hz, which is the interesting bandwidth for the motivated automotive applications (force feedback, steering position control for SbW and vehicle state estimation). For the parameter identification, the steering system is connected to an electric linear motor simulating a linear spring-damper behaviour for the rack force F_r or, for a second identification process, the rack force is excited with the linear motor and the EPS motor works as a spring-damper load to prevent of to much drift of the steering rack. The steering wheel is freely oscillating without any additional torque input ($T_{ha} = 0$ Nm). The sweep starts at a frequency of 0 Hz and the frequency gradient is 0.1 Hz/s. In general, all system models can adopt the real behaviour in the analysed frequency range (in case of an 1-mass system, there is no T_{sen} signal because of the rigid connection between rack and column). As we can see from the frequency domain result of the real system, some of the natural frequencies are in the frequency range of interest, e.g. the first at 1 Hz and the second at about 2.4 Hz. The most important fact is the great match of the 4-mass, the 3-mass and the 2-mass system for the complete frequency range. Only the 1-mass model shows a small inaccuracy in the results. So, we conclude that the stiffness of the torque sensor in the column and the inertia of the steering wheel are important parts to influence the characteristics of the system. In contrast to the stiffness c_{be} and c_{sc}, the value for c_{sen} is well known as it is a measurement device. Thus, for a rack force estimation algorithm, a well reasoned model selection is necessary, because a higher order model (e.g. 4-mass model) requires more exact parameter knowledge, computational power, and an additional application effort. Thus, the next section starts with the selection of a proper model for the estimation algorithm.

3. STEERING RACK FORCE ESTIMATION

This section deals with the rack force observer (RFO) algorithm. First, a proper system model from the previous section is selected. A friction compensation module is derived to transform the selected non-linear model to a linear one. Then, a linear disturbance observer is proposed to extract the disturbance from the model input and measurement signals. The performance of the estimation process is analysed by means of the validated 4-mass model, the real EPS on the test-bench, and a real production car (BMW 3 series).

3.1 Selection of a system model for model-based estimation

The main focus of the rack force estimation is a real-time capable algorithm. In fact, the model order needs to be as small as possible, because the required calculation power depends in general on the model order. As we could see from the previous section, the different reduced models can follow the real system in the frequency range of interest. Obviously, the lowest order model to use is the 1-mass model. The disadvantage of this simple model is the unknown inertia of the steering wheel, if a driver provides the steering wheel with an additional but unknown torque and inertia (driver hand and arm mechanics). Thus, the proposed 2-mass model avoids this drawback as it covers the driver input by the column torque sensor T_{sen}. Hence, the 2-mass model is selected as an adequate model for the rack force estimation process. Under these conditions, it is possible to remove the upper mass (namely the steering wheel and driver inertia) of the 2-mass model and to substitute its influence on the lower part with an additional input T_{sen} from the torque sensor (see Fig. 6 (right)):

$$T_{sen} = c_{sen} \left(\phi_{sw} - i_{pi} x_r \right). \tag{6}$$

Thus, we reduce the multi-input 2-mass system to a single-input system by transforming T_{sen} with the ratio i_{pi}/i_{APA} to the rotor side of the 2-mass model. Then, we combine it with the input from the assist torque T_{em}:

$$T_{1m} = T_{em} + (i_{pi}/i_{APA})\, T_{sen}. \tag{7}$$

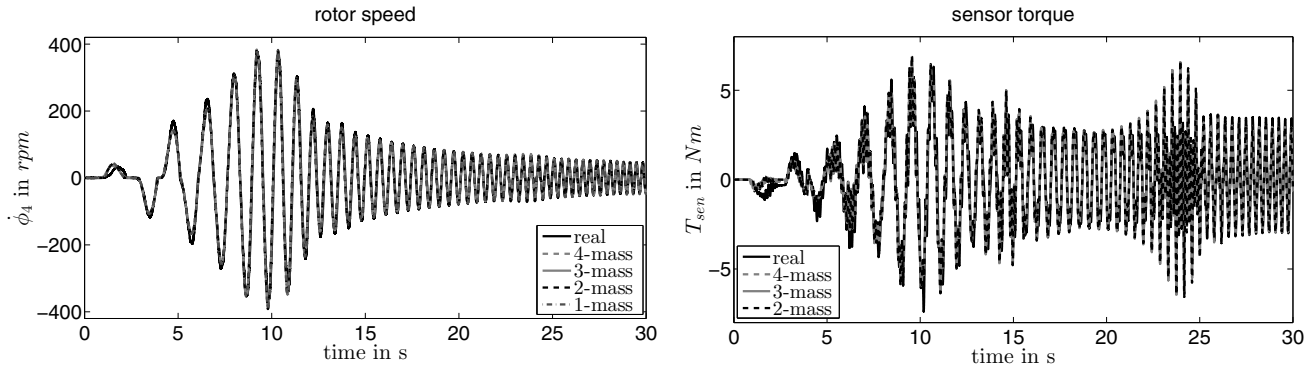

Fig. 4. Validation of the EPS models using a test-bench and sinus sweep input ($\widehat{T}_{em,r} = 0.4$ Nm from 0 Hz - 3 Hz) - time domain

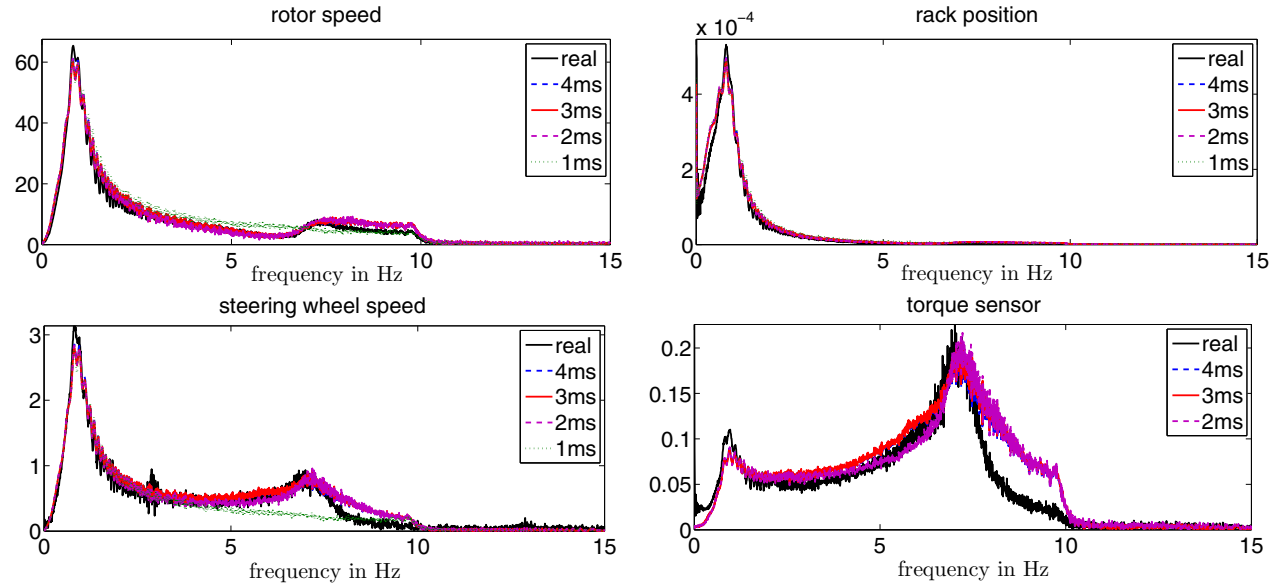

Fig. 5. Validation of the EPS models using a test-bench and sinus sweep input ($\widehat{F}_r = 750$ N from 0 Hz - 15 Hz) - frequency domain

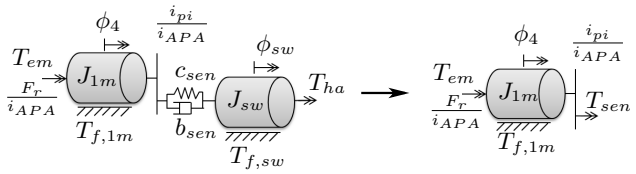

Fig. 6. Reduction of the 2-mass steering system for rack force estimation

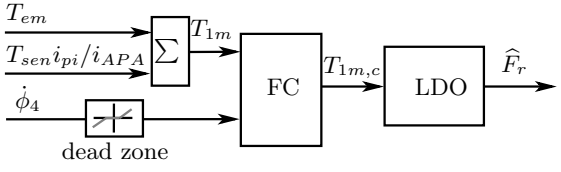

Fig. 7. Block diagram of the RFO (FC - Friction Compensation, LDO - Linear Disturbance Observer)

This means that we could reduce the 5-mass model of the steering system to a 2-mass system and with the sensor between the two remaining masses, it is possible to neglect the steering column part. Finally, we found the following non-linear 1-mass system for the rack force estimation process:

$$J_{1m} = m_r/i_{APA}^2 + (i_{li}/i_{APA})^2 J_{wh} + J_4 + (1/i_{be})^2 J_{ba} \quad (8a)$$

$$J_{1m}\ddot{\phi}_4 = T_{1m} - F_r/i_{APA} - T_{f,1m} - b_{1m}\dot{\phi}_4 \quad (8b)$$

Herein, $T_{f,1m}$ is defined as $T_{f,4}$ in eq. (5) without the damping part and with approximated parameters. The motor dynamics are neglected, as the result in Fig 4 shows that the motor ECU almost perfectly tracks the reference torque $T_{em,r}$.

3.2 Friction Compensation (FC)

Previous to the application of a linear estimation method, the non-linear friction of the steering system must be removed. Thus, a friction compensation module is introduced. It is assumed that the real friction is well approximated ($\widehat{T}_{f,1m} \approx T_{f,1m}$) and directly acting on the

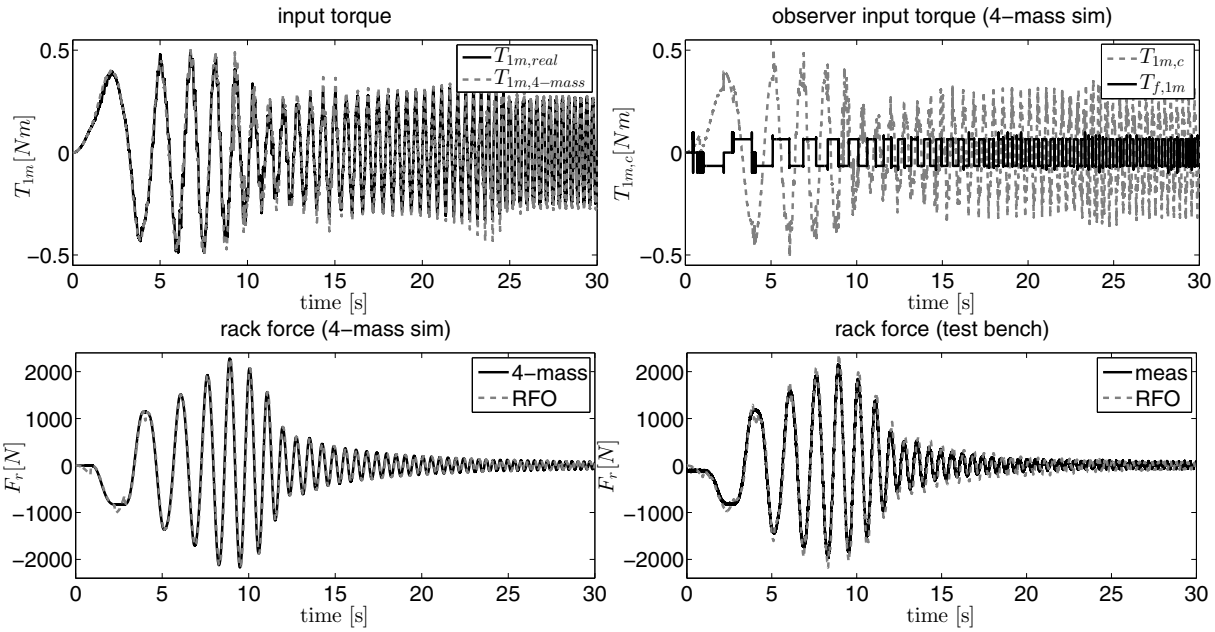

Fig. 8. Output of the friction force estimation - simulation and test-bench

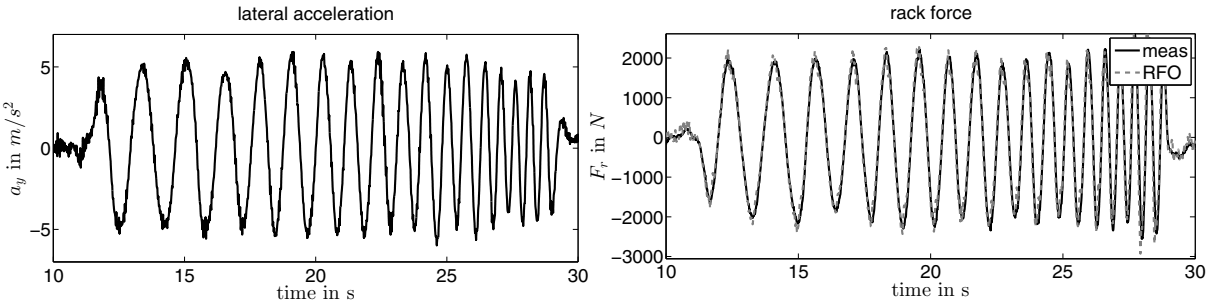

Fig. 9. Output of the non-linear friction force estimation - BMW test car with EPS at continuous speed of 70 km/h

reduced mass in eq. (8b). To improve the performance under real noisy measurement of $\dot{\phi}_4$, a dead zone element is added, which prevents of a noisy friction compensation. Consequently, the approximated friction force is added to the input of the 1-mass system and the remaining system reads

$$T_{1m,c} = T_{1m} + \widehat{T}_{f,1m} \tag{9a}$$

$$J_{1m}\ddot{\phi}_4 = T_{1m,c} - F_r/i_{APA} - b_{1m}\dot{\phi}_4 - T_{f,1m} \tag{9b}$$

Hence, input torque $T_{1m,c}$ compensates the non-linear friction part and only the damping and the disturbance force act on the reduced inertia J_{1m}.

3.3 Linear Disturbance Observer (LDO)

The linear system of the compensated and reduced 2-mass model in eq. (9b) allows a state-space description of the system dynamics with

$$\dot{\mathbf{x}}_s = \mathbf{A}_s\mathbf{x}_s + \mathbf{B}_s u_s + \mathbf{E}_s d_s \tag{10a}$$

$$\mathbf{y}_s = \mathbf{C}_s\mathbf{x}_s \tag{10b}$$

and the elements

$$\mathbf{x}_s = \begin{bmatrix}\phi_4 \\ \dot{\phi}_4\end{bmatrix}, \quad u_s = T_{1m,c}, \quad \mathbf{y}_s = \begin{bmatrix}\phi_4 \\ \dot{\phi}_4\end{bmatrix}, \tag{11a}$$

$$\mathbf{A}_s = \begin{bmatrix}0 & 1 \\ 0 & -\dfrac{b_{1m}}{J_{1m}}\end{bmatrix}, \quad \mathbf{B}_s = \begin{bmatrix}0 \\ \dfrac{1}{J_{1m}}\end{bmatrix}, \quad d_s = F_r, \tag{11b}$$

$$\mathbf{E}_s = \begin{bmatrix}0 \\ \dfrac{-1}{i_{APA}J_{1m}}\end{bmatrix}, \quad \mathbf{C}_s = \begin{bmatrix}1 & 0 \\ 0 & 1\end{bmatrix}. \tag{11c}$$

For the design of the disturbance observer, one more state is added to the state vector which describes the dynamics of the disturbance. For this reason, a simple autonomous system with

$$\dot{x}_d = A_d x_d, \quad y_d = C_d x_d, \tag{12a}$$

$$x_d = F_r, \quad A_d = 0, \quad C_d = 1 \tag{12b}$$

is combined with eq. (10a)-(10b) and leads to the extended system model

$$\begin{bmatrix}\dot{\mathbf{x}}_s \\ \dot{x}_d\end{bmatrix} = \begin{bmatrix}\mathbf{A}_s & \mathbf{E}_s C_d \\ 0 & A_d\end{bmatrix}\begin{bmatrix}\mathbf{x}_s \\ x_d\end{bmatrix} + \begin{bmatrix}\mathbf{B}_s \\ 0\end{bmatrix} u_s \tag{13a}$$

$$\mathbf{y} = \begin{bmatrix}\mathbf{C}_s & 0\end{bmatrix}\begin{bmatrix}\mathbf{x}_s \\ x_d\end{bmatrix}. \tag{13b}$$

With a proper selection of the feedback gain matrix $\mathbf{L}^T = [\mathbf{L}_1, \mathbf{L}_2]$ for the estimator feedback,

$$u_e = \begin{bmatrix} \mathbf{L}_1 \\ \mathbf{L}_2 \end{bmatrix} (\mathbf{y} - \widehat{\mathbf{y}}), \quad \widehat{\mathbf{y}} = [\, \mathbf{C}_s \; 0 \,] \begin{bmatrix} \widehat{\mathbf{x}}_s \\ \widehat{x}_d \end{bmatrix} \tag{14}$$

the disturbance observer state-space equation with speed sensor and position sensor feedback reads

$$\begin{bmatrix} \dot{\widehat{\mathbf{x}}}_s \\ \dot{\widehat{x}}_d \end{bmatrix} = \begin{bmatrix} \mathbf{A}_s - \mathbf{L}_1\mathbf{C}_s & \mathbf{E}_s C_d \\ -\mathbf{L}_2\mathbf{C}_s & A_d \end{bmatrix} \begin{bmatrix} \widehat{\mathbf{x}}_s \\ \widehat{x}_d \end{bmatrix} + \begin{bmatrix} \mathbf{B}_s \\ 0 \end{bmatrix} u_s + \begin{bmatrix} \mathbf{L}_1 \\ \mathbf{L}_2 \end{bmatrix} \mathbf{y}. \tag{15a}$$

A detailed derivation of this structure can be found in Franklin et al. [2010]. The feedback gain matrix is calculated by the linear quadratic estimator (LQE) method to allow for an easy variation of the weighting between the states and measurements of the system.

4. VALIDATION OF THE RACK FORCE ESTIMATION

4.1 Numerical simulation results

Fig. 8 shows the results of the numerical simulation run with the named sinus sweep input signal from 0 - 3 Hz and the 4ms model as reference. As the parameters for the observer model match the presented simulation model, the tracking of the simulated rack force by the RFO is excellent. This is not only because of the good parametrisation of the LDO, but also due to the FC module (upper right plot). The RFO algorithm follows the rack force in the complete frequency range up to 3 Hz . The same result is found for the test-bench analysis, see Fig. 8 (lower right plot). The estimation error is slightly higher for the test-bench run at the point where the system changes its moving direction and is near to zero speed. In fact, the FC is not exactly compensating the real friction since the reduction to a single mass with a single friction compensation calculation cannot match the real system because the friction parameter uncertainty for the real system is higher than for the virtual system.

4.2 Measurement results with prototype car

Additional to the test-bench analysis, the RFO algorithm is evaluated with real measurement data from a BMW 3 series car. The car is equipped with a rack assist EPS as mentioned in Fig. 1. In contrast to the test-bench evaluation, the parameters of the observers are adapted to match the higher friction of steering device. As the reference measurement is mounted to the tie rod, additional effects of the suspension and road wheels do not influence the estimation analysis. Different driving manoeuvres are used to check the observer performance in this real scenario. To follow the idea of the previous given results, Fig. 9 shows the results of a sinus sweep steering angle input at the steering wheel with a constant vehicle speed of 70 km/h. The upper left plot includes the vehicle speed, while the upper right plot gives the lateral acceleration of the car. In addition, the yaw rate of the car is given in the lower left figure. The lower right plot presents the comparison between the tie rod force measurement (meas) and the RFO. Apparently, the RFO calculation matches the amplitude and the phase of the rack force very well. As already seen in the test-bench result, only when a sign change in the system speed is present, a small estimation error is visible.

5. SUMMARY

The equipment of modern road cars with rack assist EPS leads to an improved handling and energy efficiency of the whole car and enables additional functionality as lane keeping and active return. Some of these functions base on the knowledge of the steering rack force generated by the tyres and the forces which are acting on these. The analysis of different order models of the steering system shows that the 2-mass model is capable to cover the main characteristics of the 5-mass system in the interesting frequency range of 15 Hz. As the driver hand wheel torque is unknown and the torque between rack and steering column is measured, the 2-mass model was further reduced for basic system description of the steering system. Higher order models show the same quality but for the application with a LDO an input to each mass is necessary to use a proper friction compensation. Since the complex friction of the real system fairly influences the system dynamics, the proposed steering rack force estimation algorithm uses a friction compensation to find a linear model description. The later was then used to build a linear disturbance observer. The analysis of the algorithm confirmed that the tracking of the rack force is possible and of a high quality. These results were then confirmed by the use of a steering test-bench and real car measurements. In the next step, the analysis of a non-linear observer method is in focus of the steering rack force estimation to improve the estimation performance in case of parameter uncertainty.

REFERENCES

T. Weiskircher, S. Müller. Nonlinear State Estimation of Vehicle Dynamics for a Road Vehicle with Independent Rim-Mounted Electric Drives. *11th International Symposium on Advanced Vehicle Control*, Seoul, 2012.

C. Dannöhl, S. Müller, H. Ulbrich. H_∞-control of a rack-assisted electric power steering system. *Vehicle System Dynamics*, Taylor & Francis, Vol. 50:4, p. 527-544, 2012.

T. Weiskircher, S. Müller. Kombinierte Schätzung von Fahrzuständen und Fahrzeugparametern mittels Unscented Kalman Filter und virtueller Sensoren. *AUTOREG 2013*, Baden-Baden, Germany, 2013.

S. Fankem, S. Müller. A new model to compute the desired steering torque for steer-by-wire vehicles and driving simulators. *23rd International Symposium in Dynamics of Vehicles on roads and Tracks*, Qingdao, China, 2013.

H. Hsu, M. Harrer, S. Grüner, A. Gaedke. The New Steering System in the 911 Porsche Carrera - Optimized Design of a Steering System for Sportcars. *21st Aachen Colloquium Automobile and Engine Technology*, Aachen, Germany, 2012.

T. Koch. Untersuchungen zum Lenkgefühl von Steer-By-Wire Lenksystemen. *Dissertation, Technische Universität München*, München, Germany, 2010.

J. Hsu. Estimation and control of lateral tire forces using steering torque. *Thesis (Ph. D.), Stanford University*, Stanford, USA, 2009.

G. F. Franklin, J. D. Powell, and A. Emami-Naeini. Feedback Control of Dynamic Systems. Pearson Prentice Hall, New Jersey, 6th edition, 2010.